Research Square

Preprints are preliminary reports that have not undergone peer review.
They should not be considered conclusive, used to inform clinical practice,
or referenced by the media as validated information.

Spatiotemporal variations in groundwater and evaporative demand drive ecophysiological functioning of a phreatophyte in drylands

Maria Trinidad Torres-García (m.t.torres@ual.es)
University of Almeria: Universidad de Almeria https://orcid.org/0000-0003-2244-1758
Maria Jacoba Salinas-Bonillo
University of Almeria: Universidad de Almeria
Jamie R. Cleverly
University of Technology Sydney
Manuel Pacheco-Romero
University of Almeria: Universidad de Almeria
Javier Cabello
University of Almeria: Universidad de Almeria

Research Article

Keywords: Depth-to-groundwater gradient, ecophysiological threshold, groundwater salinity, plant functional traits, Rhamnaceae, Ziziphus lotus

Posted Date: February 17th, 2021

DOI: https://doi.org/10.21203/rs.3.rs-202180/v1

License: This work is licensed under a Creative Commons Attribution 4.0 International License.
Read Full License

Version of Record: A version of this preprint was published at Oecologia on July 31st, 2021. See the published version at https://doi.org/10.1007/s00442-021-04993-w.

Abstract

Water is the main limiting factor for groundwater-dependent ecosystems (GDEs) in drylands. Predicted climate change (precipitation reductions and temperature increases) and anthropogenic activities such as groundwater drawdown jeopardize the structure and functioning of these ecosystems, presenting new challenges for their management. We developed a trait-based analysis to examine the spatiotemporal variability in the ecophysiology of *Ziziphus lotus*, a phreatophyte that dominates one of the few terrestrial GDEs of semiarid regions in Europe. We assessed morpho-functional and hydraulic traits along a naturally occurring gradient of depth-to-groundwater (DTGW, 2–25 m) in a coastal aquifer, and throughout the growing season of the species. Increasing DTGW and salinity negatively affected photosynthetic and transpiration rates, increasing plant water stress (lower predawn and midday water potential), and positively affected Huber value (sapwood cross-sectional area per leaf area), reducing leaf area and likely, plant hydraulic demand. However, higher atmospheric evaporative demand fostered higher transpiration rates and water stress. Differences in climatic conditions throughout the growing season drove temporal variability in *Z. lotus* responses along the DTGW gradient, with warmer and drier conditions promoting carbon assimilation and water loss more intensively at shallow water tables. This multiple-trait analysis allowed us to identify plant ecophysiological thresholds related to the increase in DTGW and evaporative demand during the growing season. These findings highlight the existence of tipping points in the ecophysiological functioning of phreatophytic plants in drylands, which contribute to disentangle the functional responses of the related GDEs under groundwater detriment because of climate change effects.

1. Introduction

Water is an essential global resource for humans and ecosystems, particularly in arid regions where it is the most limiting factor (Newman et al., 2006). Arid and semiarid regions are characterized by low and shifting water availability across space and time (Eamus et al., 2013), thus vegetation has to live with water limitation or explore new water sources below ground (Arndt et al., 2001; Nardini et al., 2014). In this sense, groundwater reservoirs are crucial for the functioning of vegetation (O'Grady et al., 2006) in the ecosystems that have access to this hidden water source, the so-called groundwater-dependent ecosystems (GDEs) (Eamus et al., 2006). GDEs of arid regions are highly vulnerable to alterations in the hydrological regime, because their structure and functioning depend on it (Eamus et al., 2006). Groundwater condition, i.e., water quality and quantity, affects GDEs, and groundwater exploitation or pollution jeopardizes their structure and function as well as the species that constitute them (Zolfaghar et al., 2014; Eamus et al., 2015). How the structure and function of GDEs in arid and semiarid regions are affected by groundwater variations is a primary concern for scientists, managers, and policymakers who have to design sustainable plans to manage groundwater resources in the face of climate change (Klove et al., 2014).

Fluctuations in groundwater depth can be detrimental to the functioning of GDEs and the deep-rooted phreatophytic vegetation that tap groundwater (Naumburg, 2005). Groundwater drawdown can salinize

both soils and water in arid regions due to the exclusion of salts by plants during water uptake or to the exposure of deeper and saltier groundwater (Jobbagy and Jackson, 2007; Runyan and D'Odorico, 2010). Seawater intrusion, as an indirect effect of water table decline near the coast, is one of the main drivers of coastal aquifer salinization. Likewise, groundwater availability for plants can depend on salinity, which has shown substantial consequences in phreatophytic productivity, even inducing diebacks (Jolly et al., 1993; Doody and Overton, 2009; Runyan and D'Odorico, 2010). Even though salinity is a significant abiotic stress that intensifies drought impacts and water unavailability, there is little research on plant response to both groundwater salinity and depth (Kath et al., 2015; Hussain and Al-Dakheel, 2018; Zhang et al., 2019).

Groundwater-dependent ecosystems are among the terrestrial ecosystems most vulnerable to climate change effects, and their ability to persist will depend on the resilience of phreatophytic vegetation to groundwater decline (Hultine et al., 2020). It is widely recognized that anthropogenic activities alter the groundwater regime, either directly through groundwater exploitation or indirectly through land-use change (Eamus et al., 2015, 2016), which in turn can promote soil and groundwater salinization (Jobbagy and Jackson, 2007; Nosetto et al., 2008). Additionally, future climate change, expressed in the Mediterranean basin by a reduction in precipitation and an increase in temperature (Giorgi and Lionello, 2008), will reduce groundwater recharge and raise evapotranspiration rates. Modelling carbon-water relationships will help us predict how hydrological changes can affect GDEs in terms of survival and productivity, thus addressing human impacts (Naumburg et al., 2005; Newman et al., 2006). To test vegetation response to altered water regimes, scientists usually resort to spatial gradients of aridity, altitude, water availability, and soil nutrients, among others (Lavorel and Garnier, 2002; Wright et al., 2004; Mitchell and O'Grady, 2015). Topography, for instance, can promote gradients in water availability, which cause critical variations in plant structure and function (Williams et al., 1996). The study of a species response to reduced water availability along environmental gradients will provide insight for identifying ecophysiological thresholds in phreatophytic vegetation (Eamus et al., 2006; Froend and Drake, 2006).

Plant functional traits that refer to morphological, physiological, and phenological characteristics of the vegetation (Perez-Harguindeguy et al., 2013) provide insight about plant ecological strategies, contributing to understanding how vegetation responds to abiotic factors (Lavorel and Garnier, 2002; Mouillot et al., 2013; Nolan et al., 2017a). This "bottom-up" approach that relates plant traits to environmental gradients is a way forward for facing important ecological questions (Cornelissen et al., 2003). In GDEs, plant functional traits are the vehicle to assess different aspects of ecosystem functioning as they respond to changes in the hydrologic regime (Eamus et al., 2006). In this sense, an understanding of the connection between morpho-functional and hydraulic traits with groundwater characteristics (i.e., groundwater depth, conductivity, and temperature) will be crucial for predicting climate change effects upon GDEs.

Numerous morpho-functional traits such as Huber value (Hv), woody density, specific leaf area (SLA), and gas-exchange rates show variation across depth-to-groundwater (DTGW) gradients in arid and semiarid environments (Stromberg et al., 1996; Gazal et al., 2006; Butler et al., 2007; Carter and White, 2009;

Zolfaghar et al., 2014; Osuna et al., 2015; Sommer et al., 2016; Nolan et al., 2017a). Hydraulic traits such as water potential are strongly correlated with DTGW gradients, as shown in phreatophytic oaks, eucalyptus, and acacias from California and Western and Central Australia (Carter and White, 2009; Osuna et al., 2015; Nolan et al., 2017a). Here, we explore a GDE dominated by the phreatophyte *Ziziphus lotus* (L.) Lam. (*Rhamnaceae*) in a small coastal plain in the southeast of Spain where spatiotemporal variations in groundwater salinity and temperature were also assessed. We evaluated the relationships among a broad suite of morpho-functional and hydraulic traits including stem water potential, gas-exchange rate, intrinsic water-use efficiency (WUEi), Huber value (Hv), wood density, and specific leaf area (SLA), across a naturally occurring DTGW gradient related to distance from the coastline. We also assumed that seawater intrusion could more adversely affect plants near the coast. Thus, we hypothesized that spatiotemporal fluctuations of both groundwater availability and quality would drive differences in the ecophysiological functioning of *Z. lotus*. These differences could help us to identify ecophysiological thresholds, which will provide valuable insight to face upcoming management challenges in GDEs. To test these hypotheses, we address the following specific questions:

- Are there spatiotemporal variations in plant morpho-functional and hydraulic traits? Do these variations respond to groundwater conditions?
- Is there any discernible threshold in the ecophysiological functioning of *Z. lotus?* What factors drive the threshold?

2. Methodology

2.1. Site description

The study was conducted on a coastal plain at the western part of the Cabo de Gata-Níjar Natural Park, southeastern Spain (Fig. 1). The plain is dominated by the phreatophyte *Z. lotus* that thrives with shallow-rooted Mediterranean shrubs such as *Lycium intricatum*, *Salsola oppositifolia*, and *Withania frutescens* (Tirado, 2009). Vegetation shows a dispersed pattern with patchy distribution typical of arid and semi-arid Mediterranean regions, where *Z. lotus* is associated with biodiversity islands (Tirado, 2009). *Z. lotus* is responsible for most of the photosynthetic activity during summer, whereas the rest of the vegetation constituting the island grows in winter, entailing a replacement in the drivers of the primary productivity of the ecosystem (Guirado et al., 2018). The climate is characterized as Mediterranean and semiarid, with hot and dry summers and mild winters, and mean annual precipitation of 200 mm which is unevenly distributed during Spring and Autumn (Machado et al., 2011). The shallow aquifer upon which *Z. lotus* depends comprises Plio-Pleistocene conglomerate, with sandstone beneath it and Pliocene marine marl at the base. The geology results from the sedimentary basin of Sierra Alhamilla mountains (1000 m.a.s.l) and from marine deposits from the Quaternary period (Vallejos et al., 2018). Eight bores located along the study area form a net for groundwater observation that discerns between 3 sites (east plain, west plain, and the seasonal stream that crosses it) and shows a natural occurring DTGW gradient based on coastline distance and topography. Vegetation sampling was made on a total of 16 *Z. lotus* individuals

selected next to each bore (two per bore) (Fig. 1) in three specific periods of 2019 growing season: late-Spring (May), mid-Summer (July), and late-Summer (September).

2.2. Hydrologic and climatic measurements

Each bore contained two sensors (Hobo U20 Water level logger and Hobo U24 conductivity logger, Onset Comp. Coorp., Bourne, MA, USA) to obtain DTGW, electrical conductivity (i.e., salinity), and groundwater temperature (T_{GW}) every 15 minutes since May 2019. For regression analysis, we obtained mean values from each of the sampling periods. In the same way, we collected climatic data from Almería airport meteorological station every day (AEMET station), although just monthly precipitation (P) and mean monthly temperature (T_{air}) were used.

2.3. Hydraulic and morpho-functional traits

We measured water potential during the growing season at predawn (Ψ_{pd}) and midday (Ψ_{md}) in four stems on each of the 16 individuals using a Scholander pressure chamber (SKPM1405, Skye Instruments, Powys, UK). Measurements were taken before sunrise for Ψ_{pd} (from 06:00 to 07:00 hours in May and July and from 06:30 to 07:30 hours in September) and during the peak insolation for Ψ_{md} (between 13:00 and 14:00 hours). Mean values for each plant and period were calculated, and the maximum daily range ($\Delta\Psi_{max}$) was derived afterward as the difference between Ψ_{pd} and Ψ_{md}. We measured leaf gas exchange in 8 leaves per plants, covering all variation within the canopy, between 10:00 and 13:00 hours on the same days as water potential was measured. A portable infrared gas analyser (Li-6400XT; LI-COR Inc., Lincoln, NE, USA) was used with the following conditions in the chamber to standardise all measures: flow rate, 400 μmol s^{-1}; CO_2 concentration, 400 μmol mol^{-1}; and light intensity, 1800 μmol m^{-2} s^{-1}. Ambient temperature was kept, which varied between 25–30 ºC. We obtained photosynthetic rate (A), stomatal conductance (g_s), transpiration rate (E), vapour pressure deficit (VPD), and WUEi was calculated from the ratio between A and g_s.

Finally, we cut three branches per plant in July from which all leaves were removed. We measured sapwood cross-sectional area with a digital calliper in the base of each branch and estimated wood density as the volume of a piece of branch divided by its dry weight (after 48 h at 60ºC). We scanned all the leaves with a digital leaf-area meter (WinDIAS, Cambridge, UK) to calculate total leaf area (LA) per branch and used ten of the leaves to estimate the SLA of the plants, which represents the relationship between the LA and its dry weight (after 48 h at 60ºC). We calculated the Hv per plant from the ratio between the mean sapwood cross-sectional area to the mean LA.

2.4. Data analysis

We applied a two-way ANOVA for each groundwater characteristic and functional trait to assess intraspecific variability, both temporal (between sampling periods) and spatial (between sampling sites). Because SLA, Hv, and wood density were only measured once, we performed a one-way ANOVA for these traits. All traits were log-transformed except for water potentials due to the negative nature of their values.

We undertook Tukey's HSD post-hoc test after significant differences were found. We performed multiple bivariate linear regressions to test whether a single regression could describe individual functioning. Some regressions were made with mean values, as variability over time was not observed, whereas others were made with monthly data to detect seasonal patterns. Finally, we analysed multiple trait relationships across all variables with a principal component analysis (PCA). Traits were scaled prior to the analysis to obtain a unit variance. Spearman correlation analysis was applied, and the contribution of each trait in the PCA was assessed to select those variables that provide the best representation and improve the analysis. Because of that, SLA, WUEi, and wood density were not included in the final analysis. We performed all analyses in R 3.5.2 (R Core Team 2018).

3. Results

3.1. Spatiotemporal variations in groundwater

We observed significant differences in DTGW, salinity, and T_{GW} between sites, across the growing season, and for their interaction ($P < 0.001$; $df = 7, 4$). These variables increased during the growing season, although with different patterns. First, DTGW that ranged from 2.1 m (bore 1) to 25.4 m (bore 8) (Fig. 2a) increased across the growing season, although not substantially (Online resource 1). It was just at the inner-plain sites where an average increase of 18 cm was observed at the end of the season (bore 8). Near the coast, we observed more noticeable temporal fluctuations although these did not entail overall DTGW increments (Fig. 2b, c, d, and Online resource 1). Second, T_{GW} gradually increased during summer despite its narrow range (Online resource 1 and Online resource 2). These rises mainly affected bores with the shallowest water tables. bore 1 showed wider fluctuations, whereas bore 2, with the lowest T_{GW}, had the steepest increase. Finally, groundwater salinity, which ranged from 3360 µS/cm (bore 4) to 11000 µS/cm (bore 7), increased in bores 1, 3 and 7, but particularly in bore 7 where a rise in almost 1000 µS/cm was observed (Online resource 1 and Online resource 2). For these three groundwater properties (depth, temperature, and salinity), fluctuations were larger near the coast where water tables were shallower (bores 1 to 3) than in the other bores (Online resource 2).

3.2. Spatiotemporal variations in plant morpho-functional and hydraulic traits and their relationship with groundwater

Morpho-functional and hydraulic traits also showed significant differences between sampling periods, sites, and the interaction between them (Table 1 and Online resource 3). Overall, gas exchange (A and E) in *Z. lotus* leaves was higher in summer (July and September) and at those sites with the shallowest water tables. Regarding water loss, bores 1 to 4 (DTWG < 11.6 m) showed the highest g_s, especially during July and September when it reached 0.42 ± 0.03 mol H_2O m^{-2} s^{-1}, whereas bores 5 to 8 (DTGW > 14.0 m), the lowest values. It is also noticeable that high rates of E for plants from bores 1, 2, and 3 occurred in July and September, but also from bore 8 (25.3 m). Nevertheless, values of A showed significant differences in summer just at some locations (interaction term, $P < 0.001$). Individuals next to

bores 2 and 5 (with a DTGW of 7.3 and 14.0 m respectively) had higher photosynthetic rates in July, whereas plants near bores 6 and 8 (with 19.3 and 25.3 m respectively) showed lower values in summer (Table 1). In general, individuals next to bores 1 and 2 had the highest values of A (15.51 ± 1.12 and 24.88 ± 2.36 μmol CO_2 m^{-2} s^{-1} respectively), whereas bore 8 showed the lowest rates (7.16 ± 1.33 μmol CO_2 m^{-2} s^{-1}). However, A did not show differences between months. Contrary to A, WUEi was low at not only the shallowest water tables, but also at the deepest ones. Regarding water potential, more negative values of both Ψ_{pd} and Ψ_{md} were observed in July and September at sites with the highest DTGW (bores 5 to 8). Ψ_{pd} ranged between − 0.32 ± 0.02 MPa in May to -1.55 ± 0.09 MPa in September (at bore 2 and bore 8, respectively), whereas Ψ_{md} showed values between − 1.18 ± 0.04 MPa in May to -3.13 ± 0.10 MPa in July (bore 4 and bore 8, respectively). Hv showed significant differences across sites ($P = 0.027$) (Online resource 4). Plants at bore 1 had the lowest value of Hv (3.58 ± 0.08), whereas plants at bores 7 and 8 had the highest ones (11.40 ± 0.22 and 9.34 ± 0.84 respectively). Neither SLA nor wood density showed significant spatial variability.

Table 1 Summary of mean values of traits (± standard error) from plants next to each bore in the three sampling periods: May, July, and September. Depth-to-groundwater (DTGW) of each site is showed as well as the significant differences ($P < 0.05$) between months in each site (different letters). Photosynthetic rate (A), stomatal conductance (g_s), transpiration rate (E), intrinsic water-use efficiency (WUEi), predawn (Ψ_{pd}) and midday (Ψ_{md}) water potential, and vapour pressure deficit (VPD).

bore DTWG (m)	Month	A (µmol CO_2 m^{-2} s^{-1})	g_s (mol H_2O m^{-2} s^{-1})	E (mmol H_2O m^{-2} s^{-1})	WUEi (µmol CO_2 / mol H_2O)	Ψ_{pd} (MPa)	Ψ_{md} (MPa)	VPD (kPa)
bore 1 2.2 m	May	15.32 ± 1.69 a	0.33 ± 0.05 a	7.84 ± 0.81 a	50.53 ± 3.88 a	-0.42 ± 0.03 a	-1.74 ± 0.19 a	2.82 ± 0.04 a
	July	13.77 ± 1.87 a	0.35 ± 0.04 a	10.94 ± 1.08 b	37.92 ± 2.54 a	-0.63 ± 0.05 a	-2.33 ± 0.17 b	3.39 ± 0.06 b
	Sep	15.51 ± 1.12 a	0.32 ± 0.02 a	12.16 ± 0.67 b	48.11 ± 1.95 a	-1.08 ± 0.05 b	-2.98 ± 0.08 c	3.91 ± 0.03 b
bore 2 7.3 m	May	16.17 ± 1.77 a	0.23 ± 0.02 a	5.81 ± 0.48 a	73.84 ± 5.30 a	-0.32 ± 0.02 a	-1.23 ± 0.09 a	2.63 ± 0.04 a
	July	24.88 ± 2.36 b	0.40 ± 0.05 b	10.60 ± 1.05 b	73.52 ± 8.85 a	-0.64 ± 0.04 b	-2.49 ± 0.04 b	2.96 ± 0.06 a
	Sep	15.83 ± 1.47 a	0.32 ± 0.04 ab	14.10 ± 1.42 b	53.39 ± 3.42 b	-0.96 ± 0.07 c	-3.63 ± 0.10 c	4.78 ± 0.07 b
bore 3 8.6 m	May	11.13 ± 1.58 a	0.22 ± 0.03 a	6.41 ± 0.61 a	48.55 ± 4.31 a	-0.63 ± 0.04 a	-1.97 ± 0.15 a	2.93 ± 0.05 a
	July	9.48 ± 0.95 a	0.41 ± 0.03 b	10.95 ± 0.74 b	23.96 ± 2.34 b	-0.86 ± 0.06 b	-2.26 ± 0.17 a	2.87 ± 0.08 a
	Sep	11.08 ± 1.52 a	0.42 ± 0.03 b	11.89 ± 0.68 b	25.96 ± 2.94 b	-1.08 ± 0.08 c	-1.94 ± 0.17 a	3.09 ± 0.06 a
bore 4 11.6 m	May	14.34 ± 1.40 a	0.25 ± 0.03 a	6.74 ± 0.61 a	61.69 ± 5.37 a	-0.41 ± 0.04 a	-1.18 ± 0.04 a	2.82 ± 0.07 a
	July	13.68 ±1.57 a	0.38 ± 0.04 b	10.99 ± 0.85 b	35.62 ± 1.98 b	-0.55 ± 0.03 a	-1.95 ± 0.15 b	3.09 ± 0.09 a
	Sep	10.57 ± 1.26 a	0.22 ± 0.03 a	5.73 ± 0.59 a	52.29 ± 4.37 ab	-0.96 ± 0.07 b	-2.52 ± 0.23 c	2.91 ± 0.13 a
bore 5 14.0 m	May	6.84 ± 0.98 a	0.14 ± 0.01 a	3.67 ± 0.36 a	49.67 ± 4.01 a	-0.76 ± 0.05 a	-1.66 ± 0.07 a	2.71 ± 0.03 a
	July	13.26 ± 1.09 b	0.16 ± 0.01 a	7.45 ± 0.54 b	87.32 ± 8.69 b	-1.28 ± 0.09 b	-2.83 ± 0.08 b	4.68 ± 0.04 b
	Sep	10.12 ± 1.75 ab	0.24 ± 0.02 b	7.14 ± 0.42 b	40.64 ± 4.87 a	-1.29 ± 0.04 b	-2.74 ± 0.14 b	3.08 ± 0.05 a
bore 6 19.3 m	May	15.07 ± 1.56 a	0.25 ± 0.03 a	6.28 ± 0.73 a	67.19 ± 6.30 a	-0.46 ± 0.03 a	-1.44 ± 0.08 a	2.61 ± 0.04 a
	July	8.35 ± 1.50 b	0.22 ± 0.03 a	8.26 ± 0.92 a	37.20 ± 2.29 b	-1.31 ± 0.05 b	-2.98 ± 0.14 b	4.09 ± 0.06 b
	Sep	9.67 ± 1.64 b	0.24 ± 0.02 a	8.11 ± 0.53 a	39.70 ± 5.70 b	-1.24 ± 0.05 b	-1.96 ± 0.16 c	3.50 ± 0.05 b
bore 7 25.0 m	May	12.13 ± 1.42 a	0.16 ± 0.02 a	4.43 ± 0.41 a	75.87 ± 4.01 a	-0.60 ± 0.07 a	-1.64 ± 0.15 a	2.88 ± 0.04 a
	July	12.33 ± 1.20 a	0.17 ± 0.01 a	7.25 ± 0.53 b	72.17 ± 2.42 a	-1.23 ± 0.08 b	-2.79 ± 0.11 b	4.23 ± 0.07 b
	Sep	13.27 ± 1.41 a	0.32 ± 0.03 b	6.91 ± 0.43 b	41.47 ± 2.24 b	-1.19 ± 0.07 b	-2.51 ± 0.08 b	2.23 ± 0.03 a
bore 8	May	10.74 ± 1.26	0.22 ± 0.03 a	5.47 ± 0.53 a	51.91 ± 5.19	-0.43 ±	-1.36 ± 0.08	2.56 ± 0.05

		a			a	0.05 a	a	a
25.3 m	July	11.52 ± 1.52 a	0.26 ± 0.03 a	10.71 ± 0.68 b	44.52 ± 4.93 a	-1.01 ± 0.08 b	-3.13 ± 0.10 b	4.44 ± 0.14 b
	Sep	7.16 ± 1.33 b	0.29 ± 0.02 b	10.38 ± 0.54 b	23.77 ± 4.09 b	-1.55 ± 0.09 c	-3.06 ± 0.08 b	3.63 ± 0.09 c

Morpho-functional and hydraulic traits significantly responded to spatiotemporal variations. First, bivariate linear regressions revealed a weak negative relationship with DTGW for most gas-exchange traits during the growing season (Fig. 3), except for WUEi. By contrast, no relationship was observed between these traits and groundwater salinity (Online resource 5). Regarding hydraulic traits, Ψ_{pd} was the only variable that showed a significant linear relationship to both DTGW and salinity, in which Ψ_{pd} but not Ψ_{md} was significantly lower when DTGW and salinity were large (Fig. 4 and Online resource 6). Our results also showed that at large DTGW, plants had higher Hv values than when DTGW was small (Fig. 5), even though wood density and SLA did not respond to groundwater gradients (Online resource 7). Therefore, DTGW was the main variable related to spatial variation in most single morpho-functional and hydraulic traits.

Vapour pressure deficit, representing temporal variations in climatic conditions, showed a positive correlation with E during the growing season, particularly in the warm and dry summer. In May, both E and VPD showed lower values, with little variability across bores, whereas in summer (July and September), the increase in VPD was parallel to the rise in E (Fig. 6a). The general increase in VPD during the season enhanced transpiration rates more over the shallowest water tables than at the deepest ones (Fig. 6b). However, VPD did not show any significant relationship with other traits related to gas exchange (Online resource 8). The overall increment of VPD from spring to summer was related to more negative Ψ_{pd} and Ψ_{md} values, as shown in the regression analysis (Fig. 7a and b).

Temporal analysis of the relationships between traits also revealed that A, E, and g_s were positively related to each other, particularly during spring, whereas WUEi (= A / g_s) was positively related to A and negatively related to g_s in summer exclusively (Online resource 9). Our results also showed a negative relationship of Ψ_{pd} with these gas-exchange traits both in spring and summer. As water availability decreased (lower Ψ_{pd}), A, g_s, and E were reduced, but no response was observed with an increase of plant stress (lower Ψ_{md}) at any time (Online resource 9).

3.3. Multiple trait relationship for identifying ecophysiological thresholds

PCA revealed multiple trait relationships that were not identified with simple regression analysis. The two first components of the PCA explained 63.5% of the variation across plants (Fig. 8a). The first component (PC1), accounting for 37.6% of the total variation, showed strong loadings for climatic variables (i.e., T_{air}, precipitation) as well as hydraulic traits (i.e., Ψ_{pd} and Ψ_{md}) and E. The second component (PC2) explained 25.9 % of the variance and showed strong loadings for groundwater traits (particularly DTGW but also groundwater conductivity), A and g_s. Groundwater salinity and Hv also contributed to PC2, although to a

lesser extent. As a result, axis 1 showed a temporal gradient from the warmest and driest months that overlap to each other (July and September) with higher E and VPD, to the mild and humid spring (May), when water availability was higher (high Ψ_{pd}) and plant stress lower (high Ψ_{md}) (Fig. 8b). By contrast, axis 2 showed a DTGW gradient (Fig. 8c and d) where plants closer to the water table exhibited higher A and g_s but lower Hv. The PCA revealed two distinct clusters based on groundwater characteristics (DTGW, salinity) and their associated gas-exchange traits (A, g_s): one for plants at sites with shallow DTGW (< 12 m, Fig. 8c), and the other for plants at sites with deep DTGW (> 14 m, Fig. 8d).

4. Discussion

In this study, we examined the ecophysiological response of the long-lived phreatophyte *Ziziphus lotus* to a DTGW gradient, in a coastal GDE of the Mediterranean basin. We found that DTGW and salinity had a significant effect on the ecophysiological function of this phreatophyte, as hypothesised. We further found that some traits were more strongly correlated to fluctuations in DTGW and salinity (e.g., A and g_s), whereas others were more strongly related to seasonal fluctuations in climatic conditions (e.g., E, Ψ_{pd}, Ψ_{md}). By applying a multiple-trait approach, we were able to identify plant ecophysiological thresholds related to the groundwater characteristics and seasonality throughout the growing season.

4.1. Spatiotemporal variations in *Z. lotus'* morpho-functional and hydraulic traits and their relationship with groundwater

Our findings revealed spatiotemporal variations in *Z. lotus* morpho-functional and hydraulic traits, which were related to both groundwater and seasonal climatic conditions. The spatial variability in DTGW might explain the response patterns of gas exchange throughout the growing season. Increasing DTGW negatively affected carbon assimilation and water loss, as has been previously observed in a variety of GDEs (Butler et al., 2007; Carter and White, 2009; Osuna et al., 2015; Sommer et al., 2016). Thus, deep-rooted species, particularly from arid and semiarid regions, can face physiological constraints fostered by deep water sources (Nardini et al., 2014). Here, A, g_s, and E decreased with the increase in DTGW as consequence of such constraints. In summer, the importance of groundwater availability increased, as shown by the rise in these gas-exchange rates as consequence of higher net radiation and temperature (O'Grady et al., 1999; Sommer et al., 2016), and this rise in gas-exchange rates was more pronounced in plants at shallower DTGW. On the contrary, plants at deep water tables did not experience such noticeable increase in ecophysiological activity. Nevertheless, we observed that neither carbon assimilation nor water loss was compromised at any point of the growing season and at any DTGW. This result can be explained by *Z. lotus* accessing and using groundwater continuously and by avoiding stomatal closure and g_s restrictions (Torres-García et al., 2021), as demonstrated by low WUEi, not only at sites with the shallowest water tables but also at the deepest ones. Such behaviour is observed in phreatophytic vegetation with access to groundwater (Nolan et al., 2017b, 2018; Rumman et al., 2018). Additionally, *Z. lotus* transpiration rate did not decline in summer; in fact, it increased with VPD, more significantly at shallow water tables, suggesting that summer conditions could induce higher rates when sufficient

groundwater is available (Nolan et al., 2018; Eamus and Prior, 2001), and that groundwater availability to the plant depends on climatic conditions. Despite the risk of hydraulic failure due to this anisohydric behaviour (Torres-García et al., 2021) and the physiological limitations of tapping water from deep sources, *Z. lotus* plants can maintain high gas exchange under current conditions.

The naturally occurring DTGW gradient also explained the spatial variability in Ψ_{pd} and responses to differences in water availability. Ψ_{pd} largely reflects the water potential of the rooting area (Hinckley et al., 1978) and indicates groundwater access by plants when values are relatively high (Carter and White, 2009). Although *Z. lotus* plants showed values higher than − 1.55 MPa, which is high given the solute potential, we found a negative trend of Ψ_{pd} not only with increasing DTGW but also in salinity. Groundwater electrical conductivity increased with DTGW away from the coast, which could be due to a marine incursion during the Holocene that penetrated the inner parts of the plain, constituting a lagoon which dried up over time and increased the salinity of the area (Vallejos et al., 2018). This result is contrary to our assumption that seawater intrusion could affect salinity near the coast. Instead, we found that the combination of deep groundwater and high salinity away from the coast might promote water stress in the root zone (Kath et al., 2015). Physiological and even anatomical constraints to accessing deep and salty groundwater might have induced lower Ψ_{pd} and reduced water uptake despite *Z. lotus* continuous groundwater use even at these locations. Therefore, it is not a recent process of seawater intrusion that induced differences in *Z. lotus* population, but a past event that fostered different salinity conditions across the landscape.

Coupled with DTGW and salinity gradients, temporal groundwater depletion might induce water-deficit stress, particularly in the late summer (Naumburg et al., 2005; Sommer et al., 2016). Our results revealed a significant decrease in both Ψ_{pd} and Ψ_{md} from spring to summer, although DTGW did not substantially decline during the growing season. We consider that the temporal fluctuations observed in groundwater level are insufficient to induce such a response, as maximum differences reported during the growing season reached just 18 cm in bore 8. Even daily fluctuations observed at the shallowest and closer-to-the-coast sites, which can reflect groundwater use due to transpiration (Dahm et al., 2002; Thibault et al., 2017) or the effect of tides on the coastal aquifer (Vallejos et al., 2015; Levanon et al., 2017), had little effect on groundwater salinity. Thus, the significant decrease in the water potential during the growing season was due to other factors such as atmospheric evaporative demand. The negative response of both Ψ_{pd} and Ψ_{md} to increased VPD throughout the growing season shows the decisive effect of the high summer temperature on plant regulation, highlighting the importance of VPD in promoting transpiration when water availability is not limiting (Sulman et al., 2016; Amitrano et al., 2019). However, in these GDEs where daily and seasonal groundwater fluctuations are minor, phreatophytes run the risk of maximizing productivity over safety (Hultine et al., 2020), which can also be fostered by the observed anisohydric behaviour. Continued transpiration under VPD higher than 4 kPa might lead to hydraulic failure if water becomes scarce (Drake et al., 2018), which is more likely with deeper DTGW. Therefore, being an anisohydric phreatophyte in arid and semiarid regions seems to be a risky option, which can only be overcome by the resilience capacity of the plants (Hultine et al., 2020).

Different responses observed in *Z. lotus* transpiration rates could also be generated by differences in xylem traits (Attia et al., 2015). Our results revealed that Hv (the ratio of sapwood cross-sectional area to leaf area) was higher at deeper groundwater sites, as already reported for other phreatophytes of mesic (Zolfaghar et al., 2014) and xeric environments (Carter and White, 2009). Thus, variations in Hv with the DTGW gradient would derive from differences in leaf area instead of wood density, suggesting that plants with less reliable groundwater supply (deep DTGW) make smaller investments in leaf area than plants at shallow sites (Zolfaghar et al., 2014). This mechanism might allow *Z. lotus* to cope with reduced water availability by decreasing their hydraulic demand and, therefore, their transpiration rates at a canopy level (Gazal et al., 2006; Carter and White, 2009; Zolfaghar et al., 2014). Indeed, reductions of aboveground biomass are acknowledged to be a common adaptation when plants cannot overcome the anatomical and functional adaptation cost of water scarcity (Naumburg, 2005). In contrast to Hv, wood density was largely independent of groundwater because it depends on development of modified cell types (e.g., xylem vessels, fibres) (Lachenbruch and McCulloh, 2014). Likewise, our results showed that SLA was independent of DTGW, as has been reflected in some studies along water availability gradients (Nolan et al., 2017a). In this case, as SLA refers to the ratio of leaf area to leaf dry mass, or the inverse of leaf thickness (Pérez-Harguindeguy et al., 2013), SLA would be conserved as an adaptation to light levels and aridity. By contrast, leaf area reductions are medium-to-long-term adaptations to limit water loss (Zolfaghar et al., 2014; Garrido et al., 2018) that *Z. lotus* might have developed to address DTGW coupled to weak stomatal control (i.e., anisohydry). Despite being able to explain the variability of morpho-functional and hydraulic traits, the weak but significant relationships obtained revealed how difficult it is to define the functioning of a complex ecosystem like a GDE by a single regression for a given pair of traits.

4.2. Ecophysiological thresholds and future considerations

Assessing the expression of multiple traits provides tools to predict patterns of change in GDEs in response to variability in groundwater and across seasons (Hultine et al., 2020). A multiple-trait analysis revealed that the variability observed in the functioning of *Z. lotus* could be explained by the combination of both temporal variations in climatic conditions during the growing season of the species and the spatial differences in groundwater characteristics of the study area. Temporal differences from spring to summer showed a decrease in water potential with increased transpiration rates, promoted by environmental conditions (lower humidity, higher temperatures, and evaporative demand). This response could have fostered evaporative cooling, regulating leaf temperature for maintaining the plant carbon balance (Drake et al., 2018) and suggesting the decline in water potential was insufficient to indicate water stress. Thus, *Z. lotus* plants could avoid extreme thermal stress that can damage the photosynthetic machinery whilst preventing a steep decline in photosynthetic rate. However, sufficient water availability is required to maintain evaporative cooling, which is essential under ongoing increases of both mean air temperatures and the severity of heat waves (Urban et al., 2017).

By contrast to temporal fluctuations in ecophysiology, the ecophysiological functioning of *Z. lotus* across space was explained by the combination of groundwater availability (mainly determined by DTGW) and

salinity (expressed by electrical conductivity). Salinity is commonly present in arid ecosystems with phreatophytic vegetation because of reduced precipitation, which prevents leaching of salts, and evaporation, which leaves salts behind (Glen et al., 2013). We found that the DTGW gradient coincided with a salinity gradient such that the deepest groundwater was also saltiest. Without the ability to discriminate between these characteristics, we observed that higher groundwater salinity combined with larger DTGW affected the ecophysiology of *Z. lotus* and promoted remarkable differences along the naturally occurring gradient. We identified a response threshold at 12–14 m, mainly promoted by differences in gas-exchange rates, which is consistent with previous studies about the species (Torres-García et al., 2021). Saltier and deeper groundwater have a substantial effect on plants, reducing water uptake, and diminishing gas exchange (Kath et al., 2015). Such threshold might point to the DTGW limits for maintaining high ecophysiological functioning and productivity and could be used as a baseline for managing this GDE.

Under predicted climate change for semiarid regions of the Mediterranean basin, anisohydric phreatophytes like *Z. lotus* would increase their transpiration rates as well as the risk of hydraulic failure despite their relative drought tolerance (McDowell et al., 2008). For the related GDE, this means that an increase in groundwater discharge and associated increases in DTGW could also promote salinization (Jobbagy and Jackson, 2007; Runyan and D'Odorico, 2010). The expected decrease in precipitation will not support recharge or salt leaching, and salinization can continue until it reaches the tolerance threshold of the species. Once salinity intolerance is reached, further groundwater uptake will be compromised, along with plant survival (Nosetto et al., 2008). Furthermore, the ongoing reduction of groundwater would result in ecosystem-scale changes in plant rooting depth, and hydraulic and functional traits (Hultine et al., 2020). The concern is also whether a depletion in groundwater level would exceed the root growth rate (Orellana et al., 2012), or even if temporal fluctuations would have a long-term impact on plant ecophysiology. In this sense, phreatophytes that obtain groundwater from deep water tables and that already experience physiological constraints (e.g., over 14 m in the case of *Z. lotus*), could be intensively jeopardized by groundwater variations in the future.

5. Conclusions

In this research, we assessed spatiotemporal variations both in groundwater properties of a GDE in a semiarid region and in the morpho-functional and hydraulic traits of the phreatophyte that dominates this ecosystem: *Ziziphus lotus*. The naturally occurring DTGW gradient and associated monitoring field station have provided an interesting scenario to assess ecophysiological differences related to water availability for phreatophytic vegetation. Here, we show that both groundwater depth and salinity are highly connected to the ecophysiological functioning of phreatophytic vegetation in drylands. Nevertheless, no evidence of seawater intrusion seemed to affect *Z. lotus* plants, and groundwater salinity could be related to past events of seawater rise. Differences in climatic conditions throughout the growing season drove temporal variability in *Z. lotus* response, with summer conditions promoting carbon assimilation and water loss in this winter deciduous phreatophyte, more intensively at shallow water tables. The multiple-trait analysis led to identifying spatial and temporal ecophysiological

thresholds that depend on both groundwater availability and atmospheric evaporative demand. Under the expected reductions in groundwater reservoirs as consequence of both climate aridification, and the increase in groundwater consumption and drawdown by human overexploitation, understanding the structure and functioning of GDEs of arid and semiarid regions and defining ecophysiological thresholds of their phreatophytic vegetation will provide valuable insight to face upcoming management challenges.

Declarations

Acknowledgements

The authors thank Professor Juan Gisbert from the UAL for groundwater samples collection; and Emilio González Miras from the Environment and Water Agency of Andalusia for his invaluable help in the field.

Declaration

Funding: This research was done in the framework of the LTSER Platform “The Arid Iberian South East LTSER Platform - Spain (LTER_EU_ES_027)” and supported by the European project LIFE Adaptamed (LIFE14349610 CCA/ES/000612) and the RTI2018-624 102030-B-I00 project of the University of Almería (PPUENTE2020/001). MTT and MP were financially supported by a FPU Predoctoral Fellowship (16/02214 and 14/06782, respectively) of the Spanish Government. MTT also received financial support from the CEI-MAR Foundation (Campus de Excelencia Internacional del Mar).

Conflicts of interest/Competing interests: authors declare that they have no conflict of interest.

Authors' contributions: MTT, MJS, and JC conceived the study. MTT and MJS conducted fieldwork. MTT and JRC developed methodology. MTT analysed data with input of MP. MTT wrote the manuscript with input and revision of all authors.

Data availability

The dataset used during the current study is available from the corresponding author on reasonable request.

References

1. Amitrano C, Arena C, Rouphael Y et al (2019) Vapour pressure deficit: The hidden driver behind plant morphofunctional traits in controlled environments. Ann Appl Biol 175:313–325. https://doi.org/10.1111/aab.12544
2. Arndt SK, Clifford SC, Wanek W et al (2001) Physiological and morphological adaptations of the fruit tree Ziziphus rotundifolia in response to progressive drought stress. Tree Physiol 21:705–715.

https://doi.org/10.1093/treephys/21.11.705

3. Attia Z, Domec J-C, Oren R et al (2015) Growth and physiological responses of isohydric and anisohydric poplars to drought. EXBOTJ 66:4373–4381. https://doi.org/10.1093/jxb/erv195
4. Butler JJ, Kluitenberg GJ, Whittemore DO et al (2007) A field investigation of phreatophyte-induced fluctuations in the water table: Phreatophyte-induced fluctuations. Water Resour Res 43. https://doi.org/10.1029/2005WR004627
5. Carter JL, White DA (2009) Plasticity in the Huber value contributes to homeostasis in leaf water relations of a mallee Eucalypt with variation to groundwater depth. Tree Physiol 29:1407–1418. https://doi.org/10.1093/treephys/tpp076
6. Cornelissen JHC, Lavorel S, Garnier E et al (2003) A handbook of protocols for standardised and easy measurement of plant functional traits worldwide. Aust J Bot 51:335. https://doi.org/10.1071/BT02124
7. Dahm CN, Cleverly JR, Coonrod JEA et al (2002) Evapotranspiration at the land/water interface in a semi-arid drainage basin. Freshw Biol 47:831–843. https://doi.org/10.1046/j.1365-2427.2002.00917.x
8. Doody TM, Overton IC (2009) Riparian vegetation changes from hydrological alteration on the River Murray, Australia - Modelling the surface water-groundwater dependent ecosystem. In: Taniguchi M, Burnett WC, Fukishima Y et al (eds) From Headwaters to the Ocean - Hydrological Changes and Watershed Management. Taylor and Frances Group, London, pp 395–400
9. Drake JE, Tjoelker MG, Vårhammar A et al (2018) Trees tolerate an extreme heatwave via sustained transpirational cooling and increased leaf thermal tolerance. Glob Change Biol 24:2390–2402. https://doi.org/10.1111/gcb.14037
10. Eamus D, Cleverly J, Boulain N et al (2013) Carbon and water fluxes in an arid-zone Acacia savanna woodland: An analyses of seasonal patterns and responses to rainfall events. Agric For Meteorol 182–183:225–238. https://doi.org/10.1016/j.agrformet.2013.04.020
11. Eamus D, Froend R, Loomes R et al (2006) A functional methodology for determining the groundwater regime needed to maintain the health of groundwater-dependent vegetation. Aust J Bot 54:97. https://doi.org/10.1071/BT05031
12. Eamus D, Fu B, Springer AE, Stevens LE (2016) Groundwater Dependent Ecosystems: Classification, Identification Techniques and Threats. In: Jakeman AJ, Barreteau O, Hunt RJ et al (eds) Integrated Groundwater Management. Springer International Publishing, Cham, pp 313–346
13. Eamus D, Prior L (2001) Ecophysiology of trees of seasonally dry tropics: Comparisons among phenologies. In: Advances in Ecological Research. Elsevier, pp 113–197
14. Eamus D, Zolfaghar S, Villalobos-Vega R et al (2015) Groundwater-dependent ecosystems: recent insights, new techniques and an ecosystem-scale threshold response. Hydrol Earth Syst Sci Discuss 12:4677–4754. https://doi.org/10.5194/hessd-12-4677-2015
15. Froend RH, Drake PL (2006) Defining phreatophyte response to reduced water availability: preliminary investigations on the use of xylem cavitation vulnerability in Banksia woodland species.

Aust J Bot 54:173. https://doi.org/10.1071/BT05081

16. Garrido M, Silva P, Acevedo E (2016) Water Relations and Foliar Isotopic Composition of Prosopis tamarugo Phil., an Endemic Tree of the Atacama Desert Growing at Three Levels of Water Table Depth. Front Plant Sci 7. https://doi.org/10.3389/fpls.2016.00375
17. Gazal RM, Scott RL, Goodrich DC, Williams DG (2006) Controls on transpiration in a semiarid riparian cottonwood forest. Agric For Meteorol 137:56–67. https://doi.org/10.1016/j.agrformet.2006.03.002
18. Giorgi F, Lionello P (2008) Climate change projections for the Mediterranean region. Global Planet Change 63:90–104. https://doi.org/10.1016/j.gloplacha.2007.09.005
19. Glenn EP, Nagler PL, Morino K, Hultine KR (2013) Phreatophytes under stress: transpiration and stomatal conductance of saltcedar (Tamarix spp.) in a high-salinity environment. Plant Soil 371:655–673. https://doi.org/10.1007/s11104-013-1803-0
20. Guirado E, Alcaraz-Segura D, Rigol-Sánchez JP et al (2018) Remote-sensing-derived fractures and shrub patterns to identify groundwater dependence. Ecohydrology 11:e1933. https://doi.org/10.1002/eco.1933
21. Hinckley TM, Lassoie JP, Running SW (1978) Temporal and spatial variations in water status of forest trees. For Sci 24:1–72
22. Hultine KR, Froend R, Blasini D et al (2020) Hydraulic traits that buffer deep-rooted plants from changes in hydrology and climate. Hydrol Process 34:209–222. https://doi.org/10.1002/hyp.13587
23. Hussain MI, Al-Dakheel AJ (2018) Effect of salinity stress on phenotypic plasticity, yield stability, and signature of stable isotopes of carbon and nitrogen in safflower. Environ Sci Pollut R 25:23685–23694. https://doi.org/10.1007/s11356-018-2442-z
24. Jobbágy EG, Jackson RB (2007) Groundwater and soil chemical changes under phreatophytic tree plantations. J Geophys Res 112:G02013. https://doi.org/10.1029/2006JG000246
25. Jolly ID, Walker GR, Thorburn PJ (1993) Salt accumulation in semi-arid floodplain soils with implications for forest health. J Hydrol 150:589–614. https://doi.org/10.1016/0022-1694(93)90127-U
26. Kath J, Powell S, Reardon-Smith K et al (2015) Groundwater salinization intensifies drought impacts in forests and reduces refuge capacity. J Appl Ecol 52:1116–1125. https://doi.org/10.1111/1365-2664.12495
27. Kløve B, Ala-Aho P, Bertrand G et al (2014) Climate change impacts on groundwater and dependent ecosystems. J Hydrol 518:250–266. https://doi.org/10.1016/j.jhydrol.2013.06.037
28. Lachenbruch B, McCulloh KA (2014) Traits, properties, and performance: how woody plants combine hydraulic and mechanical functions in a cell, tissue, or whole plant. New Phytol 204:747–764. https://doi.org/10.1111/nph.13035
29. Lavorel S, Garnier E (2002) Predicting changes in community composition and ecosystem functioning from plant traits: revisiting the Holy Grail. Funct Ecology 16:545–556. https://doi.org/10.1046/j.1365-2435.2002.00664.x

30. Levanon E, Yechieli Y, Gvirtzman H, Shalev E (2017) Tide-induced fluctuations of salinity and groundwater level in unconfined aquifers – Field measurements and numerical model. J Hydrol 551:665–675. https://doi.org/10.1016/j.jhydrol.2016.12.045
31. Machado MJ, Benito G, Barriendos M, Rodrigo FS (2011) 500 Years of rainfall variability and extreme hydrological events in southeastern Spain drylands. J Arid Environ 75:1244–1253. https://doi.org/10.1016/j.jaridenv.2011.02.002
32. McDowell N, Pockman WT, Allen CD et al (2008) Mechanisms of plant survival and mortality during drought: why do some plants survive while others succumb to drought? New Phytol 178:719–739. https://doi.org/10.1111/j.1469-8137.2008.02436.x
33. Mitchell P, O'Grady A (2015) Adaptation of Leaf Water Relations to Climatic and Habitat Water Availability. Forests 6:2281–2295. https://doi.org/10.3390/f6072281
34. Mouillot D, Graham NAJ, Villéger S et al (2013) A functional approach reveals community responses to disturbances. Trends Ecol Evol 28:167–177. https://doi.org/10.1016/j.tree.2012.10.004
35. Nardini A, Lo Gullo MA, Trifilò P, Salleo S (2014) The challenge of the Mediterranean climate to plant hydraulics: Responses and adaptations. Environ Exp Bot 103:68–79. https://doi.org/10.1016/j.envexpbot.2013.09.018
36. Naumburg E, Mata-gonzalez R, Hunter RG et al (2005) Phreatophytic Vegetation and Groundwater Fluctuations: A Review of Current Research and Application of Ecosystem Response Modeling with an Emphasis on Great Basin Vegetation. Environ Manage 35:726–740. https://doi.org/10.1007/s00267-004-0194-7
37. Newman BD, Wilcox BP, Archer SR et al (2006) Ecohydrology of water-limited environments: A scientific vision: OPINION. Water Resour Res 42:. https://doi.org/10.1029/2005WR004141
38. Nolan RH, Fairweather KA, Tarin T et al (2017a) Divergence in plant water-use strategies in semiarid woody species. Functional Plant Biol 44:1134. https://doi.org/10.1071/FP17079
39. Nolan RH, Tarin T, Fairweather KA et al (2017b) Variation in photosynthetic traits related to access to water in semiarid Australian woody species. Functional Plant Biol 44:1087. https://doi.org/10.1071/FP17096
40. Nolan RH, Tarin T, Rumman R et al (2018) Contrasting ecophysiology of two widespread arid zone tree species with differing access to water resources. J Arid Environ 153:1–10. https://doi.org/10.1016/j.jaridenv.2018.01.003
41. Nosetto MD, Jobbágy EG, Tóth T, Jackson RB (2008) Regional patterns and controls of ecosystem salinization with grassland afforestation along a rainfall gradient: Patterns and controls of salinization. Global Biogeochem Cycles 22, GB2015. https://doi.org/10.1029/2007GB003000
42. O'Grady AP, Eamus D, Cook PG, Lamontagne S (2006) Groundwater use by riparian vegetation in the wet - dry tropics of northern Australia. Aust J Bot 54:145. https://doi.org/10.1071/BT04164
43. O'Grady AP, Eamus D, Hutley LB (1999) Transpiration increases during the dry season: patterns of tree water use in eucalypt open-forests of northern Australia. Tree Physiol 19:591–597. https://doi.org/10.1093/treephys/19.9.591

44. Orellana F, Verma P, Loheide SP, Daly E (2012) Monitoring and modeling water-vegetation interactions in groundwater-dependent ecosystems: Groundwater-dependent ecosystems. Rev Geophys 50:. https://doi.org/10.1029/2011RG000383
45. Osuna JL, Baldocchi DD, Kobayashi H, Dawson TE (2015) Seasonal trends in photosynthesis and electron transport during the Mediterranean summer drought in leaves of deciduous oaks. Tree Physiol 35:485–500. https://doi.org/10.1093/treephys/tpv023
46. Pérez-Harguindeguy N, Díaz S, Garnier E et al (2013) New handbook for standardised measurement of plant functional traits worldwide. Aust J Bot 61:167. https://doi.org/10.1071/BT12225
47. Rumman R, Cleverly J, Nolan RH, Tarin T, Eamus D (2018) Speculations on the application of foliar 13C discrimination to reveal groundwater dependency of vegetation and provide estimates of root depth and rates of groundwater use. Hydrol Earth Syst Sci 22:4875–4889. https://doi.org/10.5194/hess-22-4875-2018
48. Runyan CW, D'Odorico P (2010) Ecohydrological feedbacks between salt accumulation and vegetation dynamics: Role of vegetation-groundwater interactions: Salt accumulation and vegetation dynamics. Water Resour Res 46: https://doi.org/10.1029/2010WR009464
49. Sommer B, Boggs DA, Boggs GS et al (2016) Spatiotemporal patterns of evapotranspiration from groundwater-dependent vegetation: Spatiotemporal Patterns of Evapotranspiration from Phreatophytes. Ecohydrol 9:1620–1629. https://doi.org/10.1002/eco.1752
50. Stromberg JC, Tiller R, Richter B (1996) Effects of Groundwater Decline on Riparian Vegetation of Semiarid Regions: The San Pedro. Arizona Ecological Applications 6:113–131. https://doi.org/10.2307/2269558
51. Sulman BN, Roman DT, Yi K et al (2016) High atmospheric demand for water can limit forest carbon uptake and transpiration as severely as dry soil: VPD control of gpp and transpiration. Geophys Res Lett 43:9686–9695. https://doi.org/10.1002/2016GL069416
52. Thibault JR, Cleverly JR, Dahm CN (2017) Long-term water table monitoring of Rio Grande riparian ecosystems for restoration potential amid hydroclimatic challenges. Environ Manage 60:1101–1115. https://doi.org/10.1007/s00267-017-0945-x
53. Tirado R (2009) 5220 Matorrales arborescentes con Ziziphus (*). In VV.AAaa., Bases ecológicas preliminares para la conservación de los tipos de hábitat de interés comunitario en España. Ministerio de Medio Ambiente, y Medio Rural y Marino. 68 p
54. Torres-García MT, Salinas-Bonillo MJ, Gázquez-Sánchez F et al., (2021) Squandering water in drylands: The water-use strategy of the phreatophyte *Ziziphus lotus* in a groundwater-dependent ecosystem. Am. J. Bot. 108(2)
55. Urban J, Ingwers MW, McGuire MA, Teskey RO (2017) Increase in leaf temperature opens stomata and decouples net photosynthesis from stomatal conductance in Pinus taeda and Populus deltoides x nigra. J Exp Bot 68:1757–1767. https://doi.org/10.1093/jxb/erx052
56. Vallejos A, Sola F, Pulido-Bosch A (2015) Processes Influencing Groundwater Level and the Freshwater-Saltwater Interface in a Coastal Aquifer. Water Resour Manage 29:679–697.

https://doi.org/10.1007/s11269-014-0621-3

57. Vallejos A, Sola F, Yechieli Y, Pulido-Bosch A (2018) Influence of the paleogeographic evolution on the groundwater salinity in a coastal aquifer. Cabo de Gata aquifer, SE Spain. J Hydrol 557:55–66. https://doi.org/10.1016/j.jhydrol.2017.12.027
58. Wright IJ, Reich PB, Westoby M et al (2004) The worldwide leaf economics spectrum. Nature 428:821–827. https://doi.org/10.1038/nature02403
59. Zhang X, Li Y, He X et al (2019) Responses of plant functional trait and diversity to soil water and salinity changes in desert ecosystem. Shengtai Xuebao/ Acta Ecologica Sinica 39:1541–1550. https://doi.org/10.5846/stxb201801300253
60. Zolfaghar S, Villalobos-Vega R, Cleverly J et al (2014) The influence of depth-to-groundwater on structure and productivity of Eucalyptus woodlands. Aust J Bot 62:428. https://doi.org/10.1071/BT14139

Figures

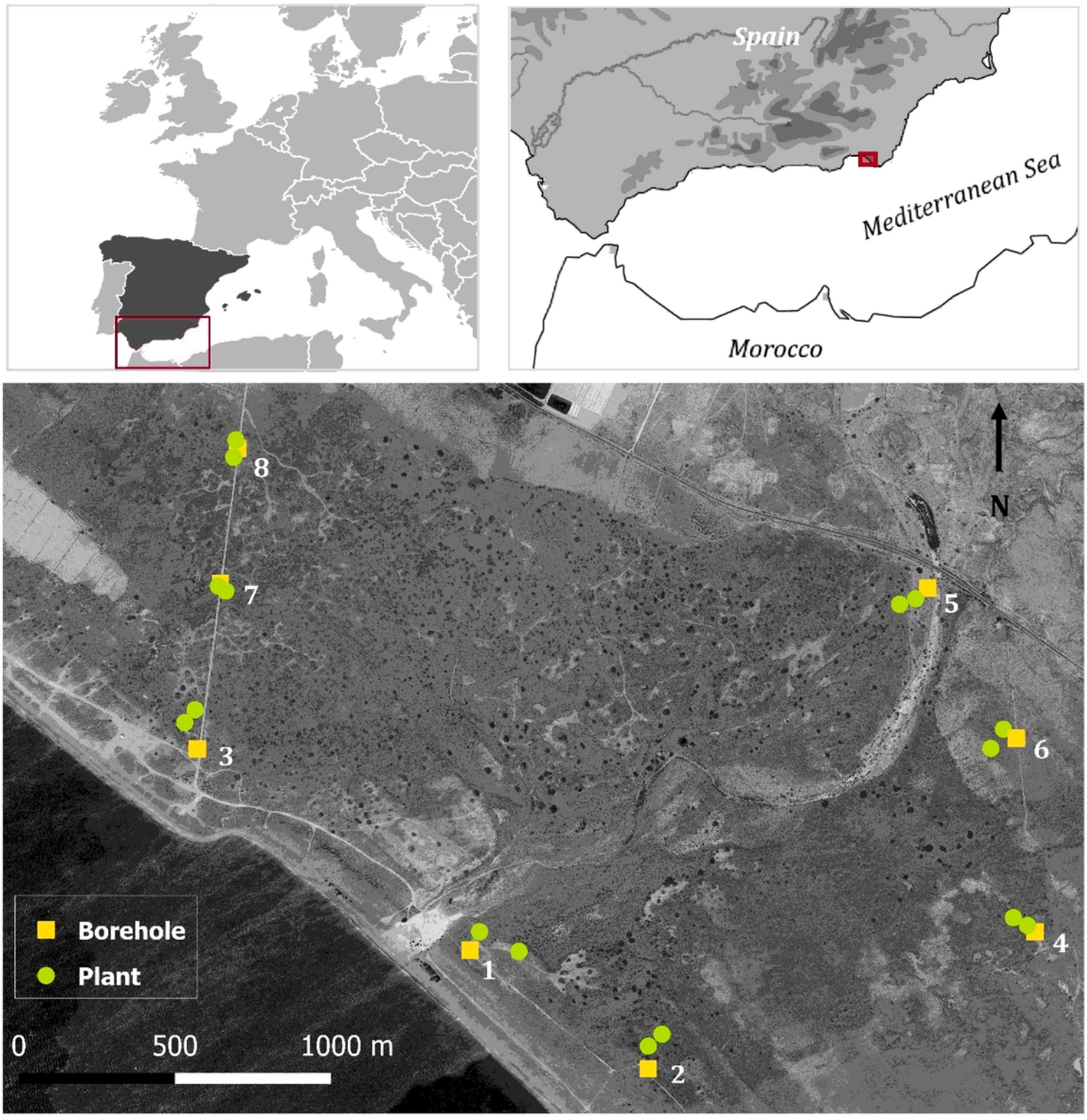

Figure 1

Distribution of the boreholes (squares 1 to 8) and the related plants of Ziziphus lotus (circles, n = 16) on the coastal plain of Cabo de Gata-Níjar Natural Park, southeastern Spain.

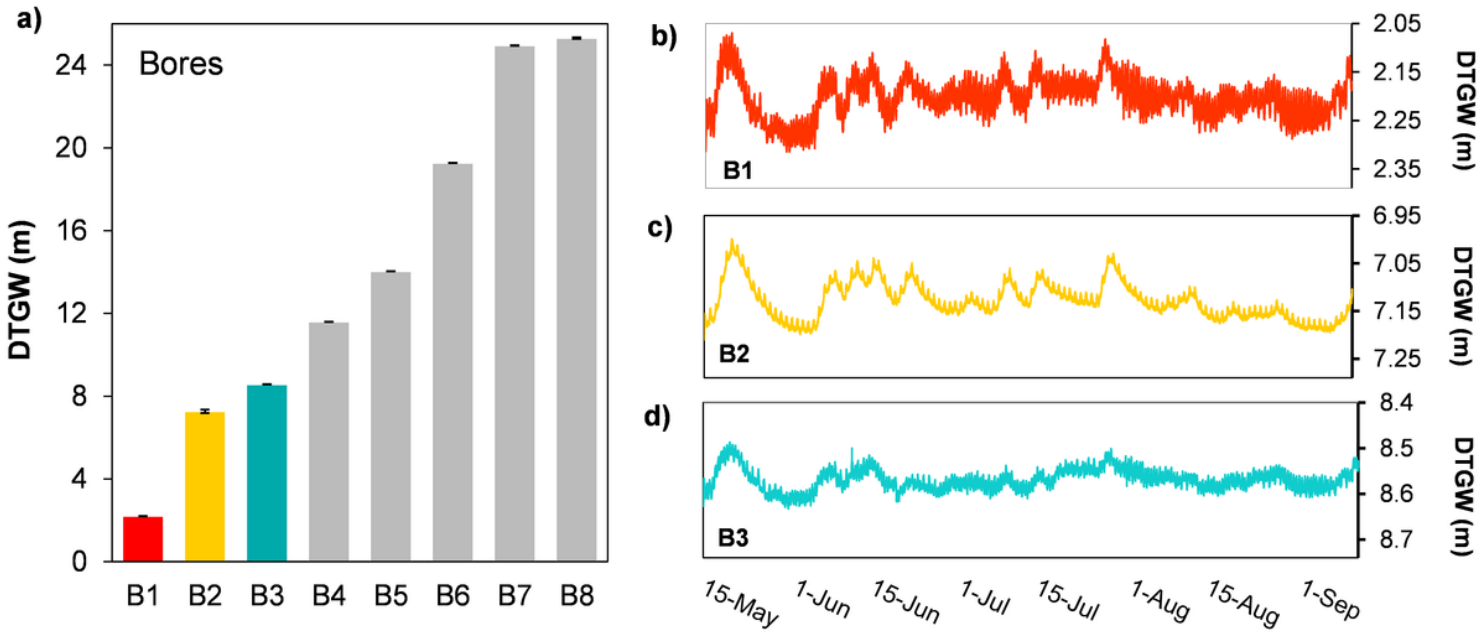

Figure 2

Mean depth-to-groundwater (DTGW, m) of the study area at different sites (bores) ± standard error (a), and temporal fluctuations in the shallowest and closest to the coast bores (b, c, and d).

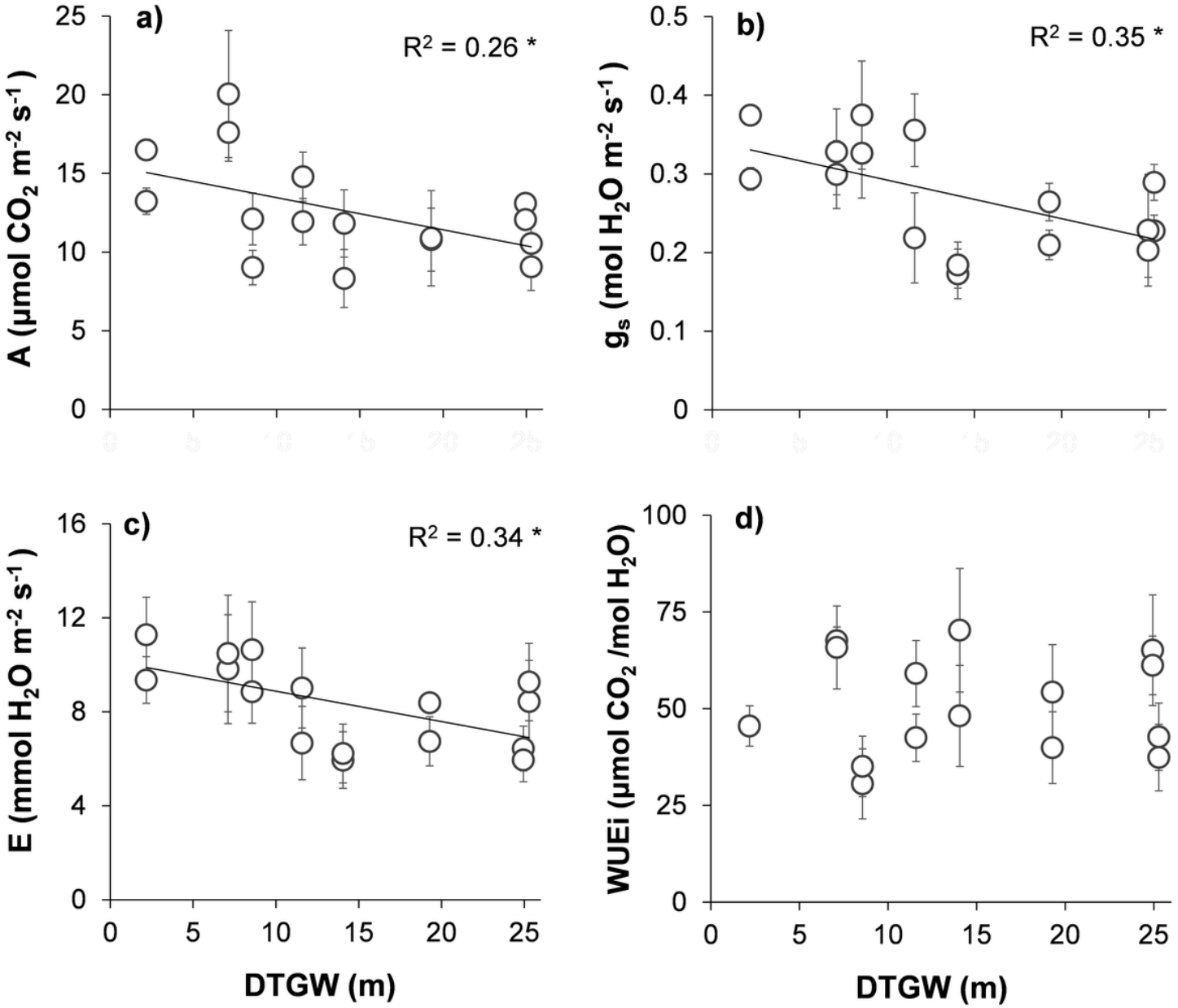

Figure 3

Bivariate linear regression between depth-to-groundwater (DTGW) and Ziziphus lotus gas exchange (photosynthetic rate, A; stomatal conductance, gs; transpiration rate, E; and intrinsic water-use efficiency, WUEi). Mean values per plant are displayed ± standard error. Lines represent significant linear regressions and R2, the goodness of the fit. Significance of the regression: *P < 0.05.

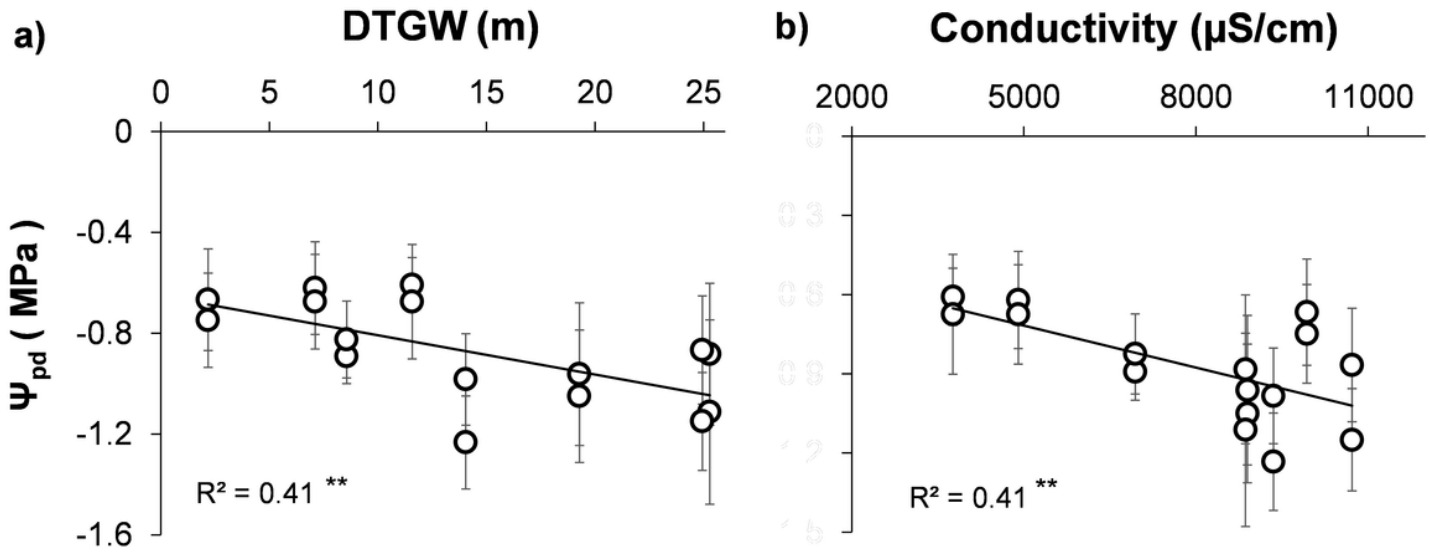

Figure 4

Bivariate linear regression between water potential at predawn (Ψpd) of Ziziphus lotus and depht-to-groundwater (DTGW) (a) and electrical conductivity (b). Mean values per plant are displayed ± standard error. Lines represent significant linear regressions and R2, the goodness of the fit. Significance of the regression: **P < 0.01.

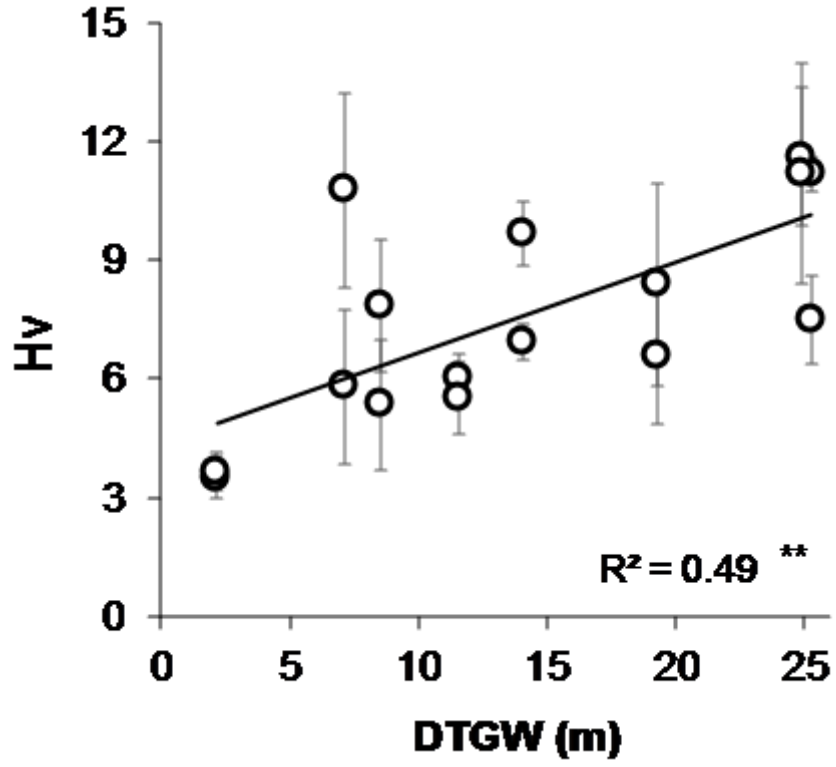

Figure 5

Bivariate linear regression between depht-to-groundwater (DTGW) and Huber value (Hv) of Ziziphus lotus. Mean values per plant are displayed ± standard error. The line represents the significant linear regression

and R2, the goodness of the fit. Significance of the regression: **P < 0.01.

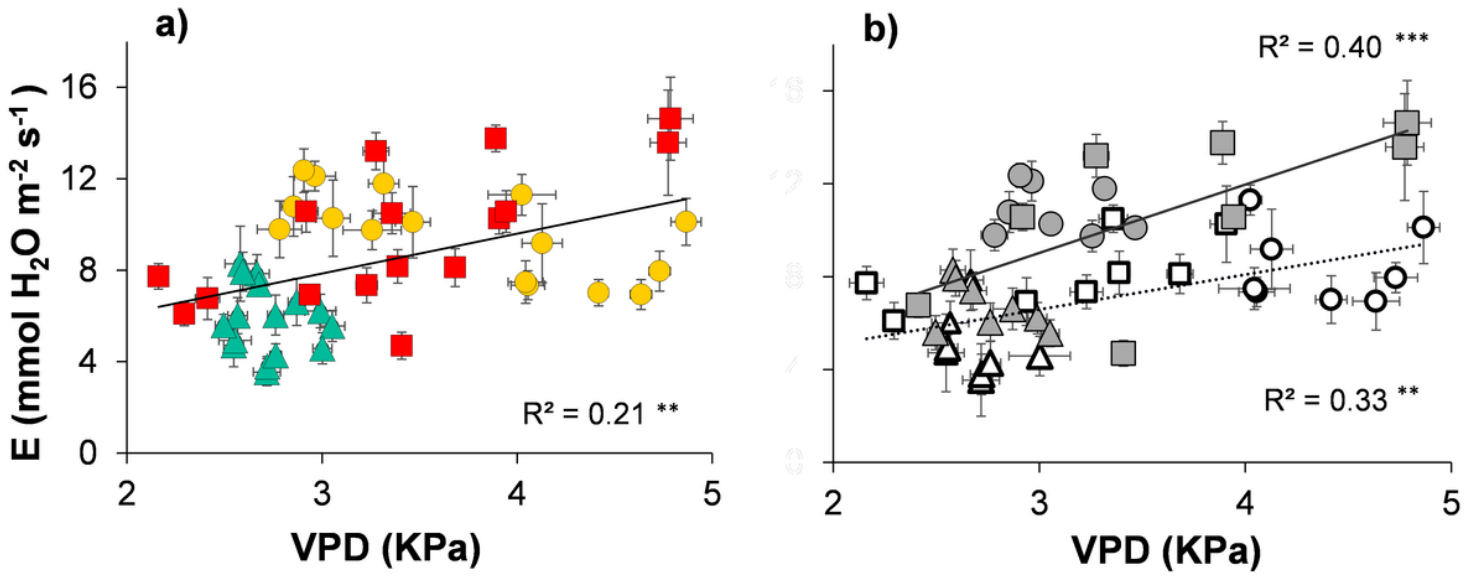

Figure 6

Bivariate linear regression between vapour pressure deficit (VPD) and transpiration rate (E) during the growing season of Ziziphus lotus. Mean values per plant are displayed ± standard error, differenciating between (a) the three sampling periods (May: green triangles, July: yellow circles, and September: red squares), (b) the three periods and shallow sites (DTGW < 12 m: grey symbols), and deep sites (DTGW > 12 m: open symbols). Significance of the regression: ***P < 0.001, **P < 0.01.

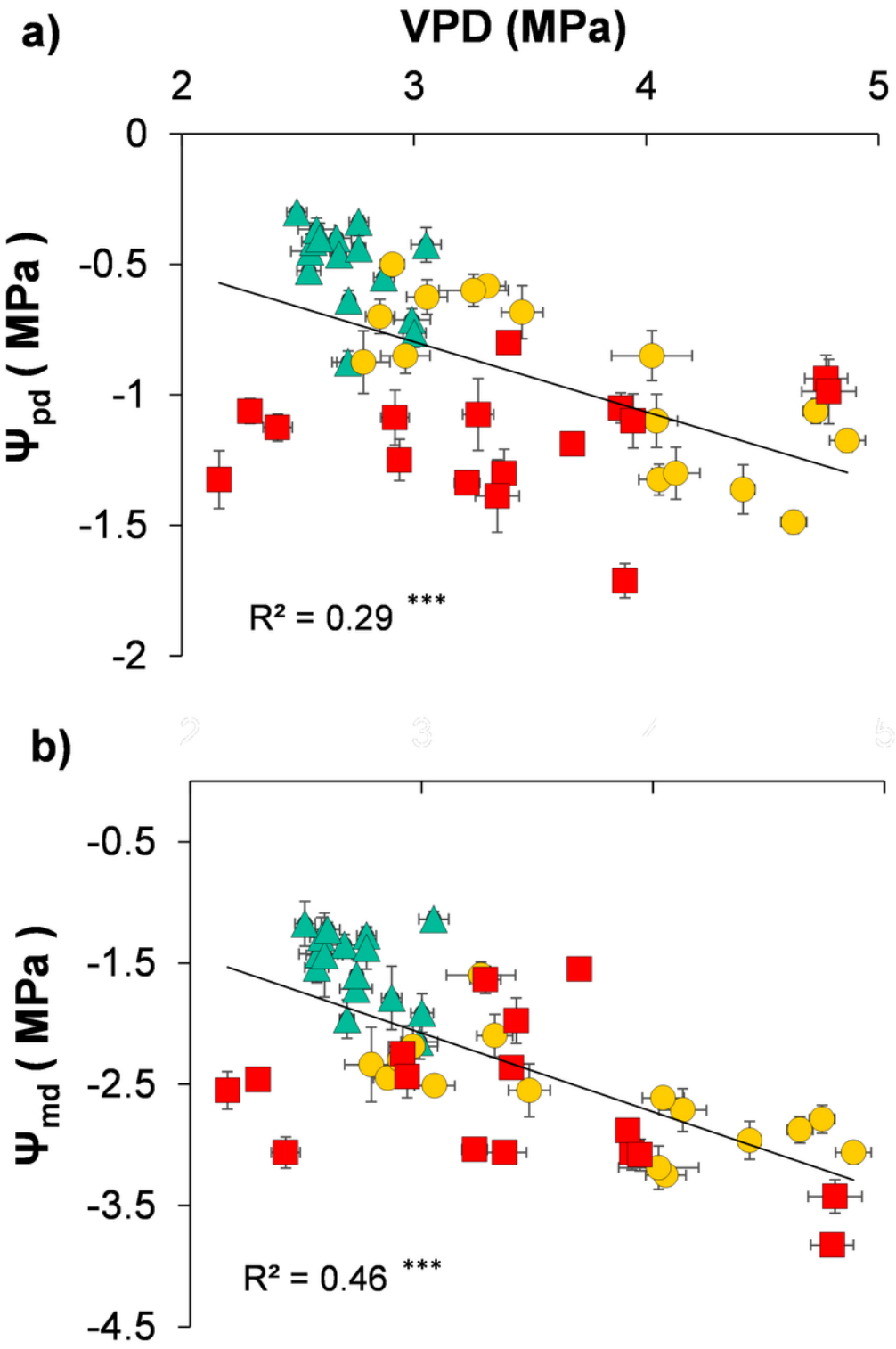

Figure 7

Bivariate linear regression between vapour pressure deficit (VPD) and predawn (a) and midday (b) water potential (Ψpd and Ψpd, respectively). Monthly values per plant are displayed ± standard error. Colours and shapes represent sampling periods: May (Green triangles), July (Yellow circles), and September (Red squares). R2 represents the goodness of the fit. Significance of the regression: ***P < 0.001.

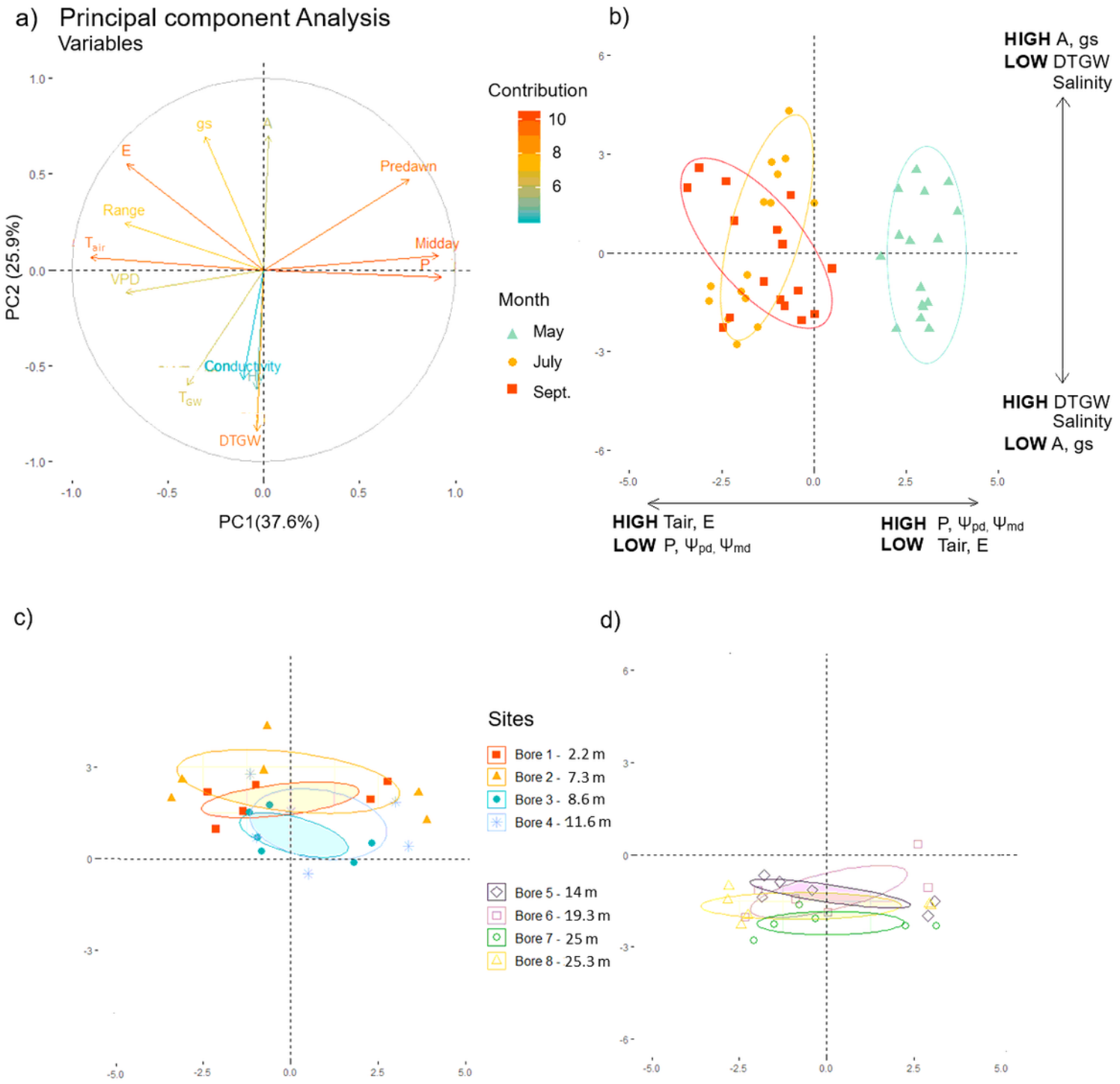

Figure 8

Principal component analysis (PCA). (a) Contribution of the variables from high (redish arrows) to low contribution (bluish arrows). (b) Representation of each individual of Ziziphus lotus in the PCA space by month (May, green triangles; July, yellow circles; and September, red squares). (c) Representation of each individual by site, differentiating between sites with DTGW lower than 12 m and (d) DTGW higher than 14

m. Horizontal and vertical arrows in panel (b) show the main variables contributing to each axis (PC1 and PC2, respectively).

Supplementary Files

This is a list of supplementary files associated with this preprint. Click to download.

- ESMTorresGarcia.docx